ZAMM · Z. Angew. Math. Mech., 1 – 9 (2013) / **DOI** 10.1002/zamm.201300001

Stress intensity factor for an infinite plane containing three collinear cracks under compression

Tao Zheng, Zheming Zhu*, Bo Wang, and Ligang Zeng

Key Laboratory of Energy Engineering Safety and Disaster Mechanics, Ministry of Education, College of Architecture and Environment, Sichuan University, Chengdu 610065, P.R. China

Received 1 January 2013, revised 9 April 2013, accepted 25 June 2013
Published online 29 July 2013

Key words Stress intensity factor, three collinear cracks, confining stress, crack surface friction.

The fracture behaviour of multi-cracked materials has become a key issue in fracture mechanics and has received large attention recently. In this paper, an infinite plane containing three collinear cracks under biaxial compression has been investigated. Considering crack surface friction and using complex stress function theory, the exact analytical solution of stress intensity factors (SIFs) for an infinite plane containing three collinear cracks is obtained. The corresponding finite element code of Abaqus is employed to validate the theoretical results, and its results agree very well with the theoretical results. The effects of confining stresses, crack distances and the crack surface frictions on SIFs are analyzed through the theoretical results and the Abaqus code. A photoelastic experiment was conducted to validate the theoretical result about the effect of confining stresses.

1 Introduction

Brittle materials usually contain a large number of cracks, such as underground rock mass and concrete, and usually they are subjected to compressive loads. Under compression, these cracks may propagate and may induce some new cracks, which will weaken brittle material strength significantly and could cause large accidents, such as rock burst and coal-gas outburst; therefore, cracks play a dominated role in structure's stability. In order to accurately predict such structure's stability so as to prevent engineering disasters, it is necessary to study the fracture behaviour of multi-cracked brittle materials under compressive loads.

Sometimes in brittle materials, the pre-existing cracks are orientated in one major direction, and they parallel each other. In this paper, the special case of collinear cracks will be investigated. Figure 1 shows a group of nearly collinear cracks in a concrete structure. These cracks affect each other, and under certain condition of loading, they will extend, branch and coalesce, and these fracturing processes have received large attention recently [1–8]. Under compression, these cracks will close and thus induce friction between crack surfaces, and the friction can resist crack surface slipping and therefore it significantly affects crack tip stress intensity factors [9–15].

The basic equations for solving the plane problems of elasticity were proposed by Muskelishvili in his famous book [16] by using complex stress functions. For the problem of an infinite plane containing multiple cracks under far field tension, solutions to the stress intensity factors (SIFs) have been obtained by a number of researchers. Fan [17] proposed a solution to the SIFs of an infinite plane containing infinite number of cracks under tension, but it's essentially different from those of infinite plane containing a finite number of cracks. By using Kachanov's approximate approach [18], Millwater [7] obtained the SIFs for an infinite plane with a group of collinear cracks under far-field tension, where the cracks length and crack spacing could be arbitrary. Li et al. [8] improved the Kachanov method by decomposing the traction in a crack into a linearly varying component and a non-uniform one so that the sum of the two components is equal to the traction along the crack length; and two or three collinear cracks in an infinite plane under far field tension were solved. Chen et al. [3] solved a variety of multi-crack problems based on integral equations and a numerical method for a cracked plane under far field tension. Although the SIFs for an infinite plane with collinear cracks have been solved by the above researchers; however, they only considered those tensile loads, and less attention has been paid to the compressive loads applied to the cracked planes. Actually the cases of cracked materials under compression exist widely in rock and concrete structures. Tensile loads mainly induce K_{I} at crack tips, whereas, compressive loads mainly induce K_{II} at crack tips, so there exists a large difference between these two kinds of loads.

* Corresponding author E-mail: zhemingzhu@hotmail.com; Tel.: 86-18628128536

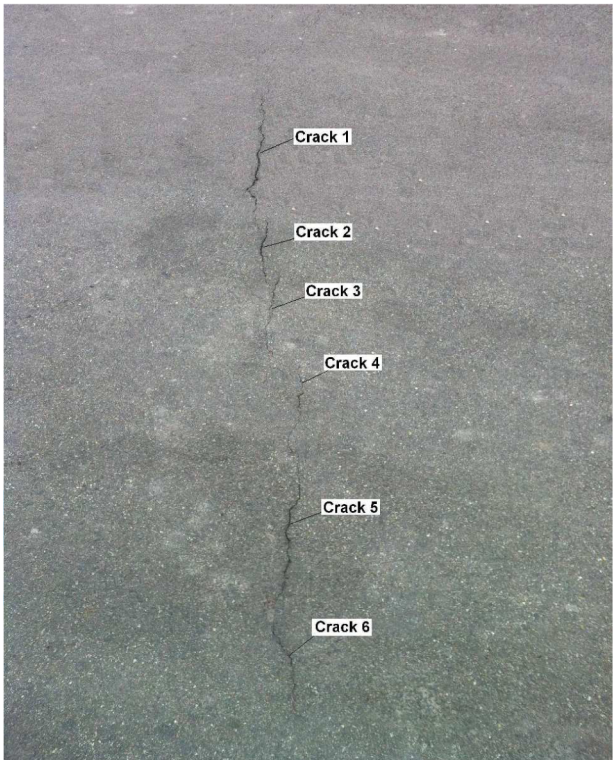

Fig. 1 A group of nearly collinear cracks existing in a concrete structure.

For the problem of a finite plane with a single crack under compression, the solution has been investigated analytically and experimentally [9–12, 19–21]. For a square plate with three collinear cracks, Jin et al. [6] obtained a semi-analytical solution of SIFs by using complex functions, and the coefficients of the complex functions were determined through boundary collocation method.

For an infinite plane contains two cracks, Basista and Gross [22] modified the Kachanov method [18] and analyzed the interaction between two cracks in brittle solids under compression. For an infinite plane containing two collinear cracks under compression, Zhu [4] obtained the accurate analytic solution of SIFs, and a new crack propagation criterion for a plane containing two collinear cracks under compression was proposed; however, for an infinite plane containing three collinear cracks, he did not give a specific analytical solution which is more complex.

In this paper, for an infinite plane containing three collinear cracks under biaxial compression, the exactly analytical solution of SIFs is presented based on Zhu's result [4], and the SIFs are obtained. The influences of confining stresses, crack surface friction and the distance between cracks on SIFs are investigated, and the corresponding finite element analysis by using Abaqus code as well as the photoelastic experiment study is implemented.

2 Formulation of stress intensity factors

In this paper, the stress intensity factors (SIFs) for an infinite plane containing three collinear cracks under compression as shown in Fig. 2 will be studied by using complex stress functions. For simplicity, three crack lengths as well as the interval distances between cracks are kept as constants. According to [16], for the elastic plane problem, the stresses can be expressed in terms of complex functions, $\Phi(z)$ and $\Omega(z)$, as

$$\sigma_{xx} + \sigma_{yy} = 4\,\mathrm{Re}[\Phi(z)] \tag{1}$$

$$\sigma_{yy} - i\sigma_{xy} = \Phi(z) + \Omega(\overline{z}) + (Z - \overline{Z})\overline{\Phi'(z)} \tag{2}$$

where $z = x + iy$. The equilibrium equations and the compatibility conditions are automatically satisfied, and the resultant force boundary condition can be expressed as

$$\phi(z) + \omega(\overline{z}) + (z - \overline{z})\overline{\Phi(z)} = i\int_{z_0}^{z}(X_n + iY_n)ds + C \tag{3}$$

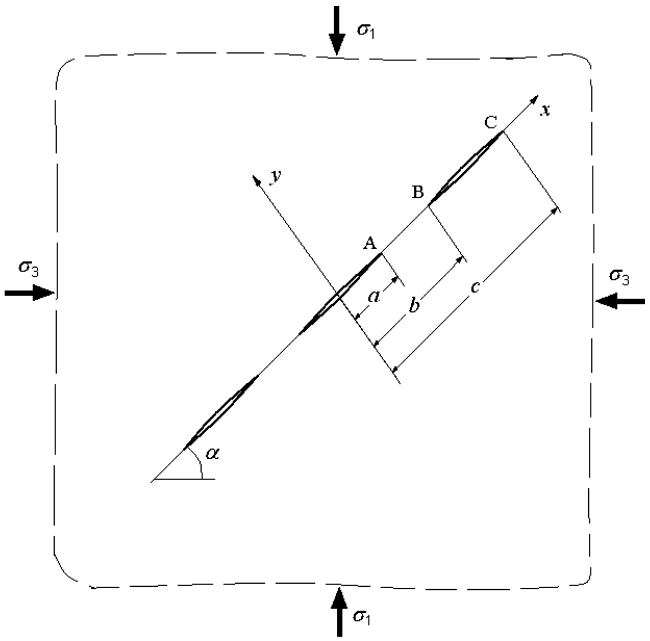

Fig. 2 A sketch of an infinite plane containing three collinear cracks under biaxial compression.

where $\varphi(z) = \int \Phi(z)dz$ and $\omega(z) = \int \Omega(z)dz$, $\bar{X}$ and $\bar{Y}$ are the boundary forces along x and y direction, respectively, and z_0 is a based point selected arbitrarily on the boundary. The displacement boundary condition can be written as

$$2G(u+iv) = \kappa\varphi(z) - \omega(\bar{z}) - (z-\bar{z})\overline{\Phi(z)} \tag{4}$$

where $\kappa = (3-\nu)/(1+\nu)$ for plane stress and $\kappa = 3-4\nu$ for plane stress, $G = E/2(1+\nu)$, E is elastic modulus, and ν is Poisson's ratio.

For the problem of an infinite plane containing collinear cracks under compression, the general formula has been presented [4, 23]. Based on the previous results, for an infinite plane containing three collinear cracks under compression as shown in Fig. 2, the complex functions $\Phi(z)$ and $\Omega(z)$ can be expressed as

$$\Phi(z) = \frac{1}{4\pi i X(z)} \int_L \frac{X^+(t)Q dt}{(t-z)} + \frac{P(z)}{X(z)} - \frac{1}{2}\bar{\Gamma}', \tag{5}$$

$$\Omega(z) = \frac{1}{4\pi i X(z)} \int_L \frac{X^+(t)Q dt}{(t-z)} + \frac{P(z)}{X(z)} + \frac{1}{2}\bar{\Gamma}', \tag{6}$$

where $P(z) = k_0 + k_1 z + k_2 z^2 + k_3 z^3$,

$$\Gamma = -\frac{1}{4}(\sigma_1 + \sigma_3),$$

$$\mathrm{Res}\left[\frac{X(\varepsilon)}{\varepsilon - z}, \infty\right] = -\mathrm{Res}\left[\frac{X(\frac{1}{\varepsilon})}{\frac{1}{\varepsilon} - z} \cdot \frac{1}{\varepsilon^2}, 0\right] = -z^3 + \frac{1}{2}(a^2+b^2+c^2)z,$$

$$k_3 = \Gamma + \frac{1}{2}\bar{\Gamma}' = -\frac{\sigma_1+\sigma_3}{4} - \frac{\sigma_1-\sigma_3}{4}(\cos 2\alpha - i\sin 2\alpha),$$

$$X(z) = \sqrt{(z^2-a^2)(z^2-b^2)(z^2-c^2)},$$

$$Q = (-1+if)[\sigma_1 + \sigma_3 + (\sigma_1 - \sigma_3)\cos 2\alpha],$$

where t is x-coordinate on crack surface, n is crack number and in this study $n = 3$, f is crack surface friction coefficient, $L = L_1 + L_2 + L_3$ is the total length of the three cracks, k_0, k_1, k_2, k_3 are constants, and σ_1, σ_3, and α are shown in Fig. 2. The integrals along L in Eqs. (5) and (6) can be expressed in terms of integrals along a closed curve C containing these three cracks [4, 24], and then Eq. (5) can be rewritten as

$$\Phi(z) = \frac{Q}{8\pi i X(z)} \int_C \frac{X(\varsigma)d\varsigma}{(\varsigma - z)} + \frac{k_0 + k_1 z + k_2 z^2 + k_3 z^3}{X(z)} - \frac{1}{2}\bar{\Gamma}'. \tag{7}$$

By using residue theory, the integral in Eq. (7) along the contour C can be expressed in terms of the sum of the residues at point z and at infinity as

$$\Phi(z)=\frac{Q}{4X(z)}\left\{X(z)+\mathrm{Res}\left[\frac{X(\varsigma)}{\varsigma-z},\infty\right]\right\}+\frac{k_0+k_1z+k_2z^2+k_3z^3}{X(z)}-\frac{1}{2}\bar{\Gamma}'. \tag{8}$$

For the three collinear cracks as shown in Fig. 2, the residue in Eq. (8) can be expressed as

$$\mathrm{Res}\left[\frac{X(\varsigma)}{\varsigma-z},\infty\right]=-\mathrm{Res}\left[\frac{X(\frac{1}{\varsigma})}{\frac{1}{\varsigma}-z}\cdot\frac{1}{\varsigma^2},0\right]=-z^3+\frac{1}{2}(a^2+b^2+c^2)z. \tag{9}$$

Substituting Eq. (9) into Eq. (8), the complex function $\Phi(z)$ can be rewritten as

$$\Phi(z)=\frac{Q}{4}+\frac{k_0+\left[\frac{Q}{8}(a^2+b^2+c^2)+k_1\right]z+k_2z^2+\left(k_3-\frac{Q}{4}\right)z^3}{X(z)}-\frac{1}{2}\overline{\Gamma}. \tag{10}$$

Because k_1 and k_3 are unknown coefficients, Eq. (10) can be simplified as

$$\Phi(z)=\frac{Q}{4}+\frac{k_0+k_1'z+k_2z^2+k_3'z^3}{X(z)}-\frac{1}{2}\overline{\Gamma}, \tag{11}$$

where $k_1'=k_1+\frac{Q}{8}(a^2+b^2+c^2)$ and $k_3'=k_3-\frac{Q}{4}$. Similarly, the complex function $\Omega(z)$ can be expressed as

$$\Omega(z)=\frac{Q}{4}+\frac{k_0+k_1'z+k_2z^2+k_3'z^3}{X(z)}+\frac{1}{2}\overline{\Gamma}. \tag{12}$$

According to the previous studies [4, 24], the single-valued displacement condition can be written as

$$(\kappa+1)\int_{L_k}[\Phi^+(t)-\Phi^-(t)]dt=0, \tag{13}$$

where L_k is the kth crack length. Substituting Eq. (11) into Eq. (13), and combining with the relation $X(t)=X^+(t)=-X^-(t)$, for the middle crack and the right crack in Fig. 2, one can have

$$\int_{-a}^{a}\frac{k_0+k_1'z+k_2z^2+k_3'z^3}{X(z)}dz=0, \tag{14}$$

$$\int_{b}^{c}\frac{k_0+k_1'z+k_2z^2+k_3'z^3}{X(z)}dz=0. \tag{15}$$

Because $X(z)$ is an even function, and the terms $k_1'z$ and $k_3'z^3$ are odd function, the corresponding integrations in Eq. (14) equal zero; and considering the fact that the cracks coincide with x-axis, i.e. $z=x$, Eq. (14) can be rewritten as

$$\int_{-a}^{a}\frac{k_0+k_2x^2}{\sqrt{(x^2-a^2)(x^2-b^2)(x^2-c^2)}}dx=0. \tag{16}$$

From Eq. (16), one can obtain $k_0=0$, $k_2=0$. Therefore, Eq. (15) can be simplified as

$$\int_{b}^{c}\frac{k_1'+k_3'x^3}{\sqrt{(x^2-a^2)(x^2-b^2)(x^2-c^2)}}dx=0, \tag{17}$$

where k_3 is known, so one can obtain k_3' by

$$k_3'=k_3-\frac{Q}{4}=\Gamma+\frac{1}{2}\bar{\Gamma}'-\frac{Q}{4}=\frac{i}{4}\{(\sigma_1-\sigma_3)\sin 2\alpha-[\sigma_1+\sigma_3+(\sigma_1-\sigma_3)\cos 2\alpha]f\}.$$

Let

$$x^2=c^2-(c^2-b^2)\sin^2\theta.$$

From Eq. (17), one can have

$$(k_1' + k_3' c^2) F\left(\frac{\pi}{2}, k\right) = k_3'(c^2 - b^2) D\left(\frac{\pi}{2}, k\right), \tag{18}$$

where $F\left(\frac{\pi}{2}, k\right) = \int_0^{\frac{\pi}{2}} \frac{d\theta}{\sqrt{1-k^2\sin^2\theta}}$ and $D\left(\frac{\pi}{2}, k\right) = \int_0^{\frac{\pi}{2}} \frac{\sin^2\theta d\theta}{\sqrt{1-k^2\sin^2\theta}}$ which are the elliptic integrals given by [25], and

$$\frac{D\left(\frac{\pi}{2}, k\right)}{F\left(\frac{\pi}{2}, k\right)} = \frac{1}{k^2} - \frac{1}{k^2} \frac{1 - \left(\frac{1}{2}\right)^2 k - \left(\frac{1}{2}\cdot\frac{3}{4}\right)^2 \frac{k^2}{3} - \left(\frac{1}{2}\cdot\frac{3}{4}\cdot\frac{5}{6}\right)^2 \frac{k^3}{5} - \cdots}{1 + \left(\frac{1}{2}\right)^2 k + \left(\frac{1}{2}\cdot\frac{3}{4}\right)^2 k^2 + \left(\frac{1}{2}\cdot\frac{3}{4}\cdot\frac{5}{6}\right)^2 k^3 + \cdots}, \tag{19}$$

where $k^2 = \frac{c^2-b^2}{c^2-a^2}$. From Eq. (18), one can obtain

$$k_1' = \frac{D\left(\frac{\pi}{2}, k\right)}{F\left(\frac{\pi}{2}, k\right)} S_0 - S, \tag{20}$$

where

$$S_0 = k_3'(c^2 - b^2) = i\frac{(c^2 - b^2)}{4}[(\sigma_1 - \sigma_3)(\sin 2\alpha - f\cos 2\alpha) - (\sigma_1 + \sigma_3) f],$$
$$S = k_3' c^2 = \frac{i}{4} c^2 [(\sigma_1 - \sigma_3)(\sin 2\alpha - f\cos 2\alpha) - (\sigma_1 + \sigma_3) f].$$

The stress intensity factors (SIFs) K_{I} and K_{II} can be expressed as

$$K_{\mathrm{I}} - iK_{\mathrm{II}} = \lim_{z\to ct} 2\sqrt{2\pi \mathrm{e}^{-i\beta}(z - ct)}\Phi(z) = \lim_{z\to ct} 2\sqrt{2\pi \mathrm{e}^{-i\beta}(z - ct)} \frac{k_1' z + k_3' z^3}{X(z)}, \tag{21}$$

where β is the crack angle with x-axis, and for the right crack tip $\beta = 0$, whereas, for the left crack tip, $\beta = \pi$, ct is the x-coordinate of crack tips (at crack tip A, $ct = a$). Because the coefficients k_1' and k_3' in Eq. (21) are pure imaginaries, the mode I factor $\mathrm{K_I}$ which corresponds to the real value in the right-hand side of Eq. (21) is zero, and therefore, the Mode II factor $\mathrm{K_{II}}$ will be focused in this paper. Substituting k_1' and k_3' into Eq. (21), one can obtain the corresponding dimensionless K_{II} at crack tips A, B, and C shown in Fig. 2 as

$$\begin{aligned}
Y_{\mathrm{II}}^A &= -\frac{1}{2\sigma_1}\sqrt{\frac{1}{2(a^2-b^2)(a^2-c^2)}}\left[\frac{D(\frac{\pi}{2},k)}{F(\frac{\pi}{2},k)}(c^2-b^2) - c^2 + a^2\right] \\
&\quad \times \{(\sigma_1 - \sigma_3)\sin 2\alpha - [\sigma_1 + \sigma_3 + (\sigma_1 - \sigma_3)\cos 2\alpha] f\}, \\
Y_{\mathrm{II}}^B &= -\frac{1}{2\sigma_1}\sqrt{\frac{b(c+b)}{b^2-a^2}}\left[\frac{D(\frac{\pi}{2},k)}{F(\frac{\pi}{2},k)} - 1\right]\{(\sigma_1 - \sigma_3)\sin 2\alpha - [\sigma_1 + \sigma_3 + (\sigma_1 - \sigma_3)\cos 2\alpha] f\}, \\
Y_{\mathrm{II}}^C &= \frac{1}{2\sigma_1}\sqrt{\frac{c(c+b)}{(c^2-a^2)}}\frac{D\left(\frac{\pi}{2},k\right)}{F\left(\frac{\pi}{2},k\right)}\{(\sigma_1 - \sigma_3)\sin 2\alpha - [\sigma_1 + \sigma_3 + (\sigma_1 - \sigma_3)\cos 2\alpha] f\},
\end{aligned} \tag{22}$$

where $Y_{\mathrm{II}} = K_{\mathrm{II}}/K_0$, $K_0 = \sigma_1\sqrt{\pi(a-b)}$, and $D\left(\frac{\pi}{2},k\right)/F\left(\frac{\pi}{2},k\right)$ can be obtained from Eq. (19).

3 Finite element analysis by using Abaqus code

In order to validate the theoretical results, i.e. Eq. (22), the corresponding finite element (FE) study by using Abaqus code is implemented. There are four ways to simulate crack issue in Abaqus code by using different models, i.e. damage initiation model, cohesive element model, XFEM model and pre-cracking model. In this simulation, the pre-cracking mode by using triangular element CPS6 and quadrilateral element CPS8 is employed. Because the theoretical results in Eq. (22) are obtained from an infinite plane containing three collinear cracks, thus the domain size in FE calculation should be much larger than the crack dimension, and in this simulation, the calculation domain is a 10 m $\times$ 10 m, and the crack length is the same and equals to 1.0 cm. The ratio of the domain dimension to crack length is 1000 which is large enough.

In order to validate the theoretical results, the calculation results by using Abaqus code are compared with the results from Eq. (22) in Fig. 3. The parameters selected: $a = 0.5$ cm, $b = 1.0$ cm, $c = 2.0$ cm (thus the crack lengths are a the same, i.e. $c - b = 2a = 1.0$ cm), $f = 0.0$. The SIF values at tips A, B, and C (shown in Fig. 2) for various ratios of σ_3/σ_1 (vary from 0 to 1.0) and various crack angles with σ_3-axis (vary from 0° to 90°) are calculated by Eq. (22) and by the corresponding Abaqus code. From Fig. 3, it can be seen that the finite element results, i.e. the dashed curves, agree very well with the theoretical results Eq. (22), i.e. the solid curves. The small error may be caused by the finite dimension in the Abaqus code, since the theoretical results by Eq. (22) are from infinite plane.

Actually, under large compression, especially as the lateral stress is very large, plastic deformation may occur, but for brittle material, such as rock, the plastic deformation is limited and very small. Therefore, in this paper, the plastic deformation is not addressed.

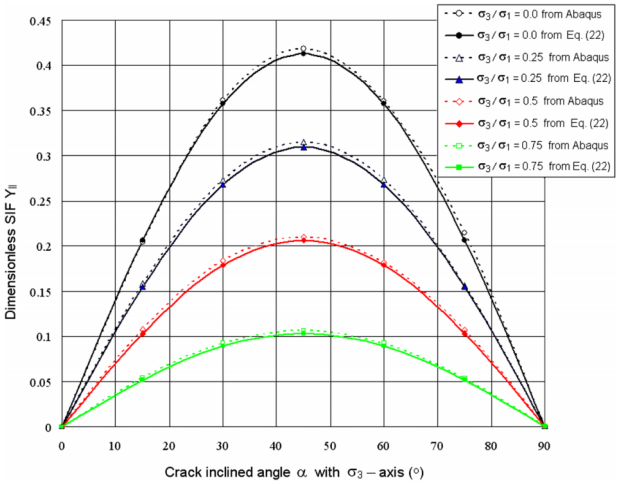

(a) Y_{II} at crack tip A

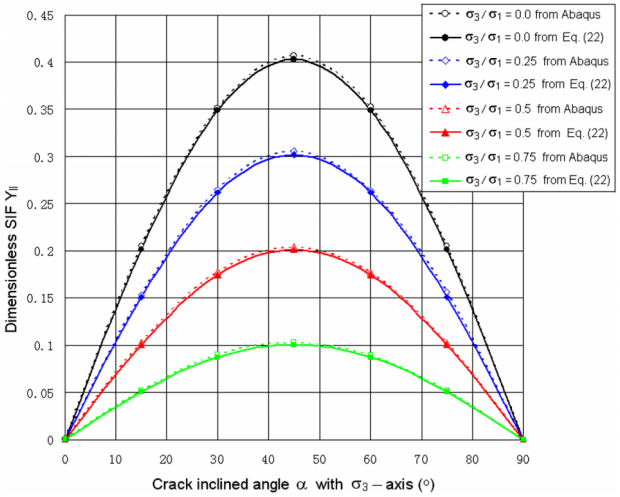

(b) Y_{II} at crack tip B

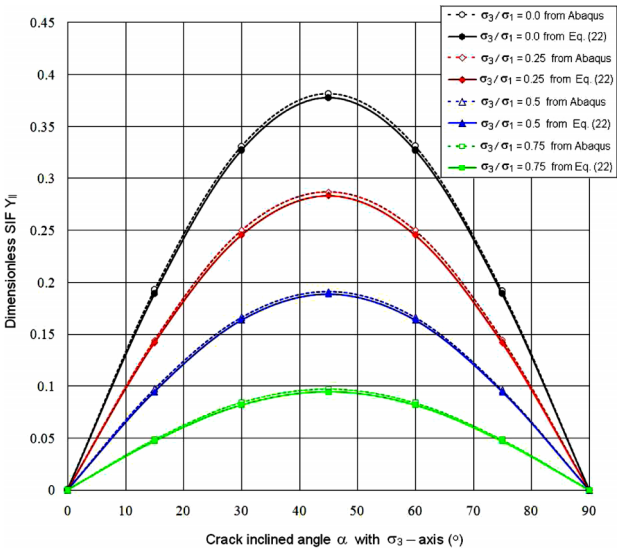

(c) Y_{II} at crack tip C

Fig. 3 The calculation results of Y_{II} for three collinear cracks under compression by using Abaqus code (dashed curves) and by the theoretical results Eq. (22).

4 The factors that affect stress intensity factors

In order to investigate the effect of confining stresses, crack distances, and crack friction coefficients on SIFs, the SIF values for various conditions are calculated from Eq. (22), from the corresponding finite element code of Abaqus, and meanwhile a photoelastic test is implemented.

4.1 The effect of confining stress on SIFs

From Fig. 3, one can find that the values of the dimensionless SIF $Y_{\rm II}$ ($Y_{\rm II} = K_{\rm II}/K_0$) generally decrease as the confining stress increases. When σ_3/σ_1 equals zero, the corresponding $Y_{\rm II}$ - α curve is the uppermost of all the curves, and when σ_3/σ_1 equals 1.0, the whole $Y_{\rm II} - \alpha$ curve merge into the α axis. The most unfavorable orientation is 45° as no friction exists between the crack surfaces. Comparing the $Y_{\rm II}$ values at crack tips A, B, and C shown in Fig. 3, it can be seen that at crack tip A, the SIF value is always the largest among the three tips, and at tip B, it is slightly higher than that at tip C.

In order to qualitatively investigate the effect of confining stress on SIFs, the corresponding photoelastic experiment using polycarbonate (PC) plates is conducted, and the test results are shown in Fig. 4. The PC plate size is 13 cm × 13 cm × 0.6 cm; the crack length is 1.0 cm; the crack width is 0.1 cm; and the crack orientation is 45°. These specimens are heated at 130°C for one hour in a vacuum drying oven before testing in order to release residual stresses. The vertical stress is kept as a constant, and the ratio of horizontal stress to vertical stress is 0.0, 0.4, and 0.8, respectively. From the photoelastic results in Fig. 4, it can be clearly seen that the order of fringes decreases as the ratio σ_3/σ_1 increase, which indicates that SIF decreases as confining stress increases, and therefore, the photoelastic results qualitatively agree with the theoretical results.

(a) $\sigma_3 / \sigma_1 = 0.0$ (b) $\sigma_3 / \sigma_1 = 0.4$ (c) $\sigma_3 / \sigma_1 = 0.8$

Fig. 4 The photoelastic results of the order of fringes for PC plates with various ratios of σ_3/σ_1; the parameters: crack length is 1.0 cm, crack tip distance is 1.0 cm, $\alpha = 45°$.

4.2 Influence of crack distance on SIFs

In order to study the influence of crack distance on SIFs, an infinite plane with three collinear cracks are considered. The ratio of σ_3/σ_1 is fixed as 0.5; the crack orientation α is fixed as 45°; the crack length is 1.0 cm; the friction coefficient f is zero; and the distance d between two adjacent crack tips varies from 0.5 cm to 5.0 cm. For different crack tip distance d, the values of $Y_{\rm II}$ at tip A, B, and C are calculated by Eq. (22) and by Abaqus code, and their results are compared in Fig. 5. It can be seen that all the SIF values at tip A, tip B and tip C decrease rapidly as the distance d increases from 0.5 cm to 1.5 cm, and after 1.5 cm, the decrease speed slows down, and after 4.0 cm, the SIF values tend towards a constant. From Fig. 5, one can also find that the finite element results agree well with the theoretical results Eq. (22).

Zhu [5] pointed out that usually cracks affect each other, but as their distance is larger than a certain value, the effect may be negligible. For an infinite plane containing a single crack under compression with the same parameters in Fig. 5, i.e. $\sigma_3/\sigma_1 = 0.5$, $\alpha = 45°$, and $f = 0$, the SIF $Y_{\rm II}$ can be obtained according to Zhu et al. [11], or can be obtained by letting the crack distance be infinite, and the result of $Y_{\rm II}$ for a single crack is 0.1768. According to the calculation results shown in Fig. 5, the relationship between the ratio of $Y_{\rm II}$ in Fig. 5 to that of the corresponding single crack and the ratio of crack tip distance to crack length is presented in Table 1.

Table 1 The ratio of crack tip distance to crack length versus the ratio of $Y_{\rm II}$ in Fig. 5 to that of single crack.

$d/(c-b)$	0.5	1.0	2.0	3.0	4.0	5.0
$Y_{\rm II}$ ratio	1.1673	1.0774	1.0302	1.0163	1.0102	1.0069

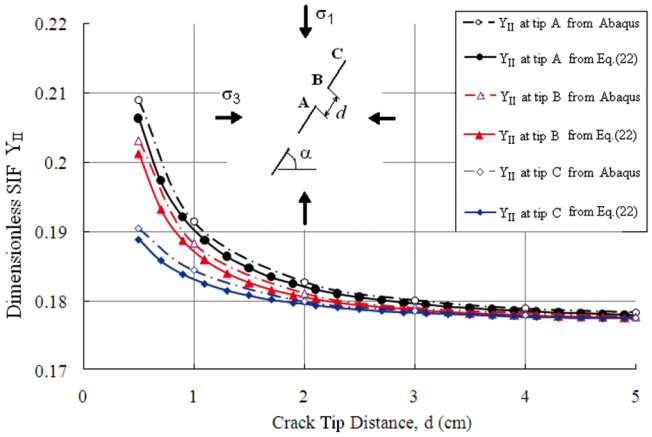

Fig. 5 The curves of $Y_{\rm II} - d$ obtained by Eq. (22) (solid curves) and by Abaqus code (dashed curves); the parameters: crack length is 1.0 cm, $\sigma_3/\sigma_1 = 0.5$, $\alpha = 45^\circ$, and $f = 0$.

From Table 1, one can find that as the ratio of crack tip distance to crack length, $d/(c-b)$, is 0.5, the SIF is 16.73% larger than the corresponding single crack's SIF value, as the ratio is 3.0, it is 1.63% larger, and as the ratio is 5.0, it is 0.69% larger. In rock engineering, 2% error is acceptable, and therefore, as crack tip distance is larger than 3 times crack length, the effect from its adjacent cracks is ignorable for three collinear cracks under compression. In Zhu [5], for two collinear crack issue, as the ratio of crack tip distance to crack length is 3.0, the SIF was 0.92% larger. This indicates the more the crack number, the more the effect from the adjacent cracks.

4.3 Influence of friction coefficient on SIFs

In order to study the influence of crack friction on SIFs, the ratio of σ_3/σ_1 is fixed as 0.2; the ratio of the distance between two crack tips to crack length is 0.5. For various crack friction coefficient f, the values of $Y_{\rm II}$ at tips A, B, and C are calculated and the results at tip A are plotted in Fig. 6. One can find that the friction coefficient has a significant effect on SIFs, and generally as the friction coefficient f increases, SIFs decrease. This is to be expected as frictions can resist crack surfaces sliding, and therefore, they can reduce crack tip SIF values. As crack friction coefficients are larger than a certain value (in Fig. 6, it is 0.9), the crack surfaces may not be able to slip, and thus the crack tip SIF values are zero, and the corresponding curve coincide with α axis.

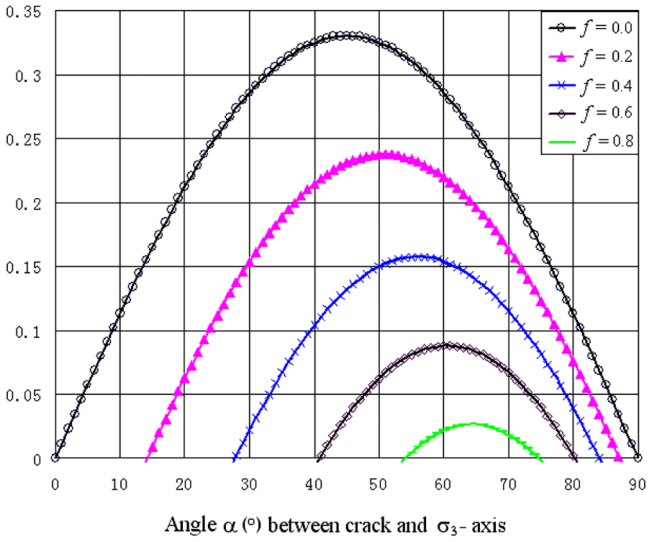

Fig. 6 The results from Eq. (22) for an infinite plane containing three collinear cracks under compression; the parameters: $\sigma_3/\sigma_1 = 0.2$, crack length is 1.0 cm, crack tip distance is 0.5 cm.

5 Conclusions

Brittle materials usually contain a large number of cracks, and they affect material strength significantly. In this paper, an infinite plane contains three collinear cracks under compression has been studied, and the corresponding formula of stress intensity factor (SIF) has been obtained by using complex stress function theory. The theoretical results have been confirmed by finite element results by using Abaqus code. By using the formula presented in this paper, the effects of confining

stresses, crack distances and crack friction coefficients on SIFs have been investigated, and a photoelastic experiment was conducted in order to confirm the theoretical result for the effect of confining stress.

The theoretical results shown in Eq. (22) can be applied to the calculation of SIF for an infinite plane containing three collinear cracks under compression, however, it is only suitable for 2D plane issue, and it cannot be employed to analyze 3D crack problem. In solving the problem of multiple collinear cracks, the difficulties are to calculate the residue $\left[\mathrm{Res}\frac{X(\varepsilon)}{\varepsilon-z},\infty\right]$ and the elliptic integrals. For the case of four or five collinear cracks, the elliptic integrals will be more difficult.

Acknowledgements This work was financially supported by the Open Fund of State Key Laboratory of Oil and Gas Reservoir Geology and Exploitation (PLN1202), by the National Natural Science Foundation of China (51074109), by the Major State Basic Research Project (2010CB732005), and by the Program for Innovative Research Team of MOE (IRT1027).

References

[1] S. X. Gong, Microcrack interaction with a finite main crack: an exact formulation, Int. J. Fract. **66**, 51–66 (1994).
[2] R. D. Wang, The stress intensity factors of a rectangular plate with collinear cracks under uniaxial tension, Eng. Fract. Mech. **56**, 347–356 (1997).
[3] Y. Z. Chen, N. Hasebe, and K. Y. Lee, Multiple Crack Problems in Elasticity (Southampton, Boston, 2003).
[4] Z. M. Zhu, An alternative form of propagation criterion for two collinear cracks under compression, Math. Mech. Solids **14**, 727–746 (2009).
[5] Z. M. Zhu, Evaluation of the range of horizontal stresses in the Earth's upper crust by using a collinear crack model, J. Appl. Geophys. **88**, 114–121 (2013).
[6] W. C. Jin, Z. M. Zhu, and M. Z. Gao, A general method to determine the stress intensity factor of multiple collinear cracks, Math. Mech. Solids, (2013), DOI: 10.1177/ 1081286512439556.
[7] H. R. Millwater, A simple and accurate method for computing stress intensity factors of collinear interacting cracks, Aerospace Sci. Technol. **14**, 542–550 (2010).
[8] Y. P. Li, L. G. Tham, Y. H. Wang, and Y. Tsui, A modified Kachanov method for analysis of solids with multiple cracks, Eng. Fract. Mech. **70**, 1115–1129 (2003).
[9] Z. M. Zhu, S. C. Ji, and H. Xie, An improved method of collocation for the problem of crack surf ace subjected to uniform load, Eng. Fract. Mech. **54**, 731–741 (1996).
[10] Z. M. Zhu, H. Xie, and S. C. Ji, The mixed boundary problems for a mixed mode crack in a finite plate, Eng. Fract. Mech. **56**, 647–655 (1997).
[11] Z. M. Zhu, L. G. Wang, B. Mohanty, and C. Y. Huang, Stress intensity factor for a cracked specimen in compression, Eng. Fract. Mech. **73**, 482–489 (2006).
[12] Z. M. Zhu, New biaxial failure criterion for brittle materials in compression, J. Eng. Mech. ASCE, **125**(11), 1251–1258 (1999).
[13] R. Ballarini and E. M. Plesha, The effects of crack surface friction and roughness on crack tip stress fields, Int. J. Fract. **34**, 195–207 (1987).
[14] A. W. Eberhardt and B. S. Kim, Crack face friction effects on mode II stress intensities for a surface-cracked coating in two-dimensional rolling contact, Tribol. Trans. **41**, 35–42 (1998).
[15] B. Lauterbach and D. Gross, Crack growth in brittle solids under compression, Mech. Mater. **29**, 81–92 (1998).
[16] N. I. Muskelishvili, Some Basic Problems of Mathematical Theory of Elasticity (Noordhoff Press, Amsterdam, 1953).
[17] T. Y. Fan, Fundamental of Fracture Theory (Science Press, Beijing, 2003), pp. 56–57.
[18] M. Kachanov, Elastic solids with many cracks: A simple method of analysis, Int. J. Solids Struct. **23**(1), 23–43 (1987).
[19] S. Nemat-Nasser and H. Horii, Compression-induced nonplanar crack extension with application to splitting, exfoliation, and rockbust, J. Geophys. Res. B **87**(8), 6805–6821 (1982).
[20] P. S. Steif, Crack extension under compressive loading, Eng. Fract. Mech. **20**, 463–473 (1984).
[21] M. F. Ashby and S. D. Hallam, The failure of brittle solids containing small cracks under compressive stress states, Acta Metall. **34**, 497–510 (1986).
[22] M. Basista and D. Gross, A note on crack interactions under compression, Int. J. Fract. **102**, 67–72, (2000)
[23] F. Erdogan, On the Stress Distribution in Plates with Collinear Cuts Under Arbitrary Loads, in: Proceedings, 4th US National Congress of Applied Mechanics, Vol. 1 (American Society of Mechanical Engineers, New York, 1962), pp. 547–553.
[24] A. H. England, Complex Variable Methods in Elasticity (Wiley-Interscience, New York, 1971).
[25] F. W. J. Olver, D. W. Lozier, R. F. Boisvert, and C. W. Clark, NIST Handbook of Mathematical Functions (Cambridge University Press, Cambridge, 2010), pp. 485-522.

